Solution structure of a synthetic lytic peptide: the perforin amino terminus

Kshama Natarajan and JA Cowan

Background: Killer lymphocytes secrete perforin, a 67 kDa protein that initiates T-cell cytolysis following aggregation and pore formation in target membranes. The resulting pores cause a breakdown of the transmembrane osmotic gradient and allow other cytolytic mediators to enter the target cell and initiate apoptosis. The cytolytic domain resides within the first 34 residues of the amino terminus of perforin, with residues 1–19 being sufficient for cytolytic activity.

Results: The solution structure of a 22-residue synthetic peptide (P_{22}), corresponding to the amino terminus of human perforin, has been determined using high resolution nuclear magnetic resonance spectroscopy in the presence and absence of perdeuterated detergent (SDS) micelles. In aqueous solution, P_{22} exists mainly in a random conformation. However, it adopts a hook-like structure at the carboxyl terminus in the presence of SDS micelles when the positively charged residues cluster to form a turn that provides a binding surface to the negatively charged sulfate headgroups.

Conclusions: The strong electrostatic interaction between the cationic region of the P_{22} peptide and the lipid headgroups probably weakens the membrane, facilitating insertion of the relatively neutral/hydrophobic stretch of P_{22}, and is representative of the initial step of the lytic pathway. The structural model described here is probably relevant to understanding the mechanisms of other cationic antimicrobial peptides.

Address: Department of Chemistry, The Ohio State University, 100 West 18th Avenue, Columbus, OH 43210, USA.

Correspondence: JA Cowan
E-mail: cowan@chemistry.ohio-state.edu

Key words: cytolysis, membrane, NMR structure, perforin, T cell

Received: **17 October 1997**
Revisions requested: **13 November 1997**
Revisions received: **5 December 1997**
Accepted: **14 January 1998**

Published: **10 March 1998**

Chemistry & Biology March 1998, **5**:147–154
http://biomednet.com/elecref/1074552100500147

Introduction

Killer lymphocytes destroy target cells using two distinct but related pathways. One mechanism arises following granule exocytosis, whereas the other follows activation of a Fas-dependent pathway [1]. For both, the effect on final cell morphology is similar, and experimental evidence suggests that the former pathway might act by triggering the latter [2]. Perforin [3,4], also known as PFP, cytolysin or C9-related protein, is a key mediator in the granule exocytosis pathway. It is 67 kDa in size, and is synthesized and localized in the granulocytes of killer lymphocytes, which contain a variety of effector proteins that serve to mediate target cell lysis [5]. After a recognition event, the contents of granulocytes are released and eventually lead to cell lysis and target cell death. Calcium is thought to trigger a conformational change in holoperforin, exposing the lytic domain, which exerts its lytic action by binding to target cell membranes, followed by oligomerization and pore formation. These pores are large enough to permit the flow of ions and low molecular weight solutes through the membrane, resulting in the disruption of ionic gradients, osmotic lysis, and cell death. Moreover, the ability of perforin to weaken and puncture cell membranes enables other lytic mediators present in granulocytes (such as proteolytic enzymes known as granzymes) to enter target cells and initiate internal signaling pathways [5].

Perforin shares both structural and functional homology with the components of the membrane attack complex [6], and in neither case is the mechanism of lymphocyte-mediated toxicity well understood. For perforin, it has been shown that lytic activity resides principally within the first 34 residues of the amino-terminal domain [7–9], although the lytic activity of the amino-terminal peptide is not calcium-dependent. Kinetic and thermodynamic studies of synthetic P_{22} (a 22-residue peptide that corresponds to the amino terminus of human perforin; Figure 1) have indicated that at least 4 ± 1 monomers are required to form functional pores in lipid vesicles [10]. To better understand the lytic function of this protein, we have determined the solution conformation of P_{22}, both in the presence and absence of sodium dodecyl sulfate (SDS) micelles. In aqueous solution, small membrane-spanning peptides do not normally possess significant tertiary structure, although a structure may exist in the presence of organic solvents or (especially) in micellar environments [11], which provide a heterologous environment that resembles a lipid bilayer. In this paper we show that the amino terminus of perforin possesses two structurally well defined regions in the presence

Figure 1

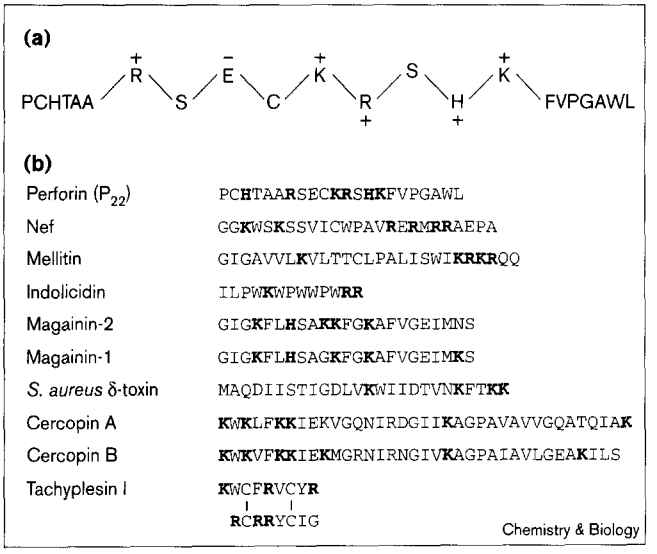

Sequences of human perforin and other lytic peptides. **(a)** Primary sequence (single-letter amino-acid code) of the amino terminus of perforin (P_{22}), highlighting the positively charged domain. **(b)** Comparison of perforin P_{22} with primary sequences for cationic antimicrobial peptide drugs. Basic residues are shown in bold type.

of SDS micelles, one of which forms a positively charged binding pocket for the negatively charged membrane, and the second, a hydrophobic domain. We propose that a strong electrostatic interaction between the charged segment of the protein and the membrane weakens the membrane and facilitates insertion of the hook-like hydrophobic structure at the carboxyl terminus of P_{22}, and represents the initial step of the lytic pathway. The structural model that we define for the amino-terminal domain of perforin in such a micellar environment should aid in understanding the interaction of the peptide with the membrane, and is likely to be relevant to understanding the mechanisms of other cationic antimicrobial peptides.

Results and discussion

NMR spectral data and constraints used for structure evaluation

Proton resonances were assigned using two-dimensional NMR techniques (correlated spectroscopy), following standard assignment procedures [12]. Figures 2 and 3 show typical one-dimensional and two-dimensional nuclear Overhauser enhancement (NOE) spectroscopy (NOESY) data. Analysis of the NOE connectivities allowed identification of secondary structure elements. Both hydrogen/deuterium (H/D) exchange data, and the presence of typical short range, medium range, and long range NOE patterns characteristic of a particular type of secondary structure, were the principal parameters used to evaluate the secondary structural features of P_{22}. Because the rotational correlation time of a micelle-bound peptide is reduced, cross relaxation is more efficient and results in a

Figure 2

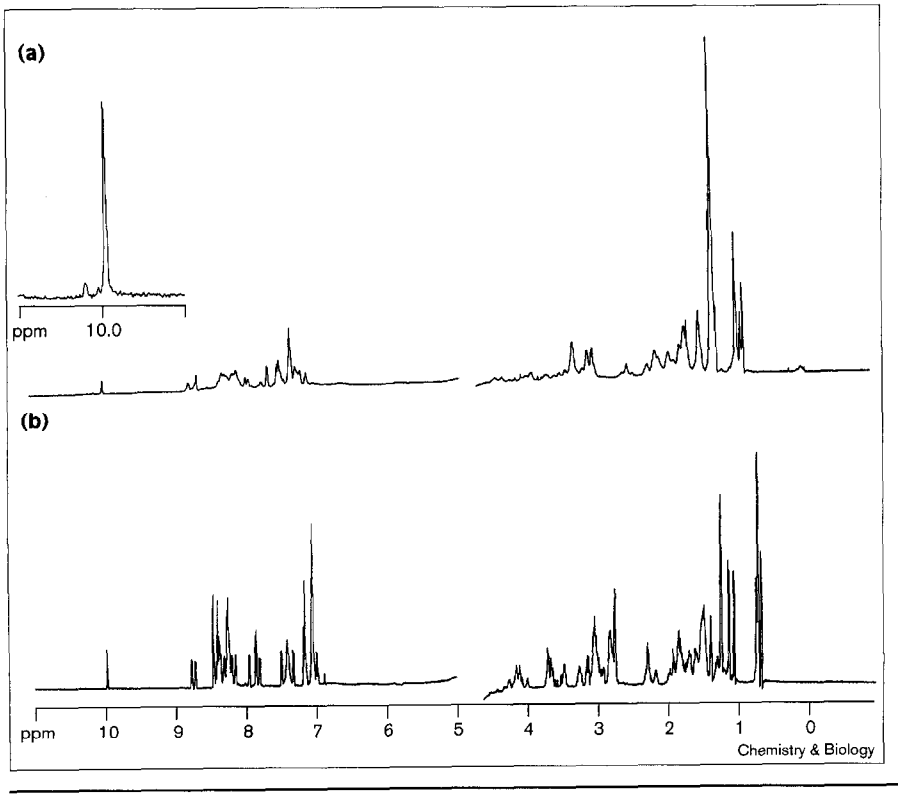

One-dimensional spectra of P_{22}. **(a)** Spectrum of P_{22} in SDS micelles. Note the duplication of tryptophan resonances in the inset. **(b)** Spectrum of P_{22} in aqueous buffer.

Figure 3

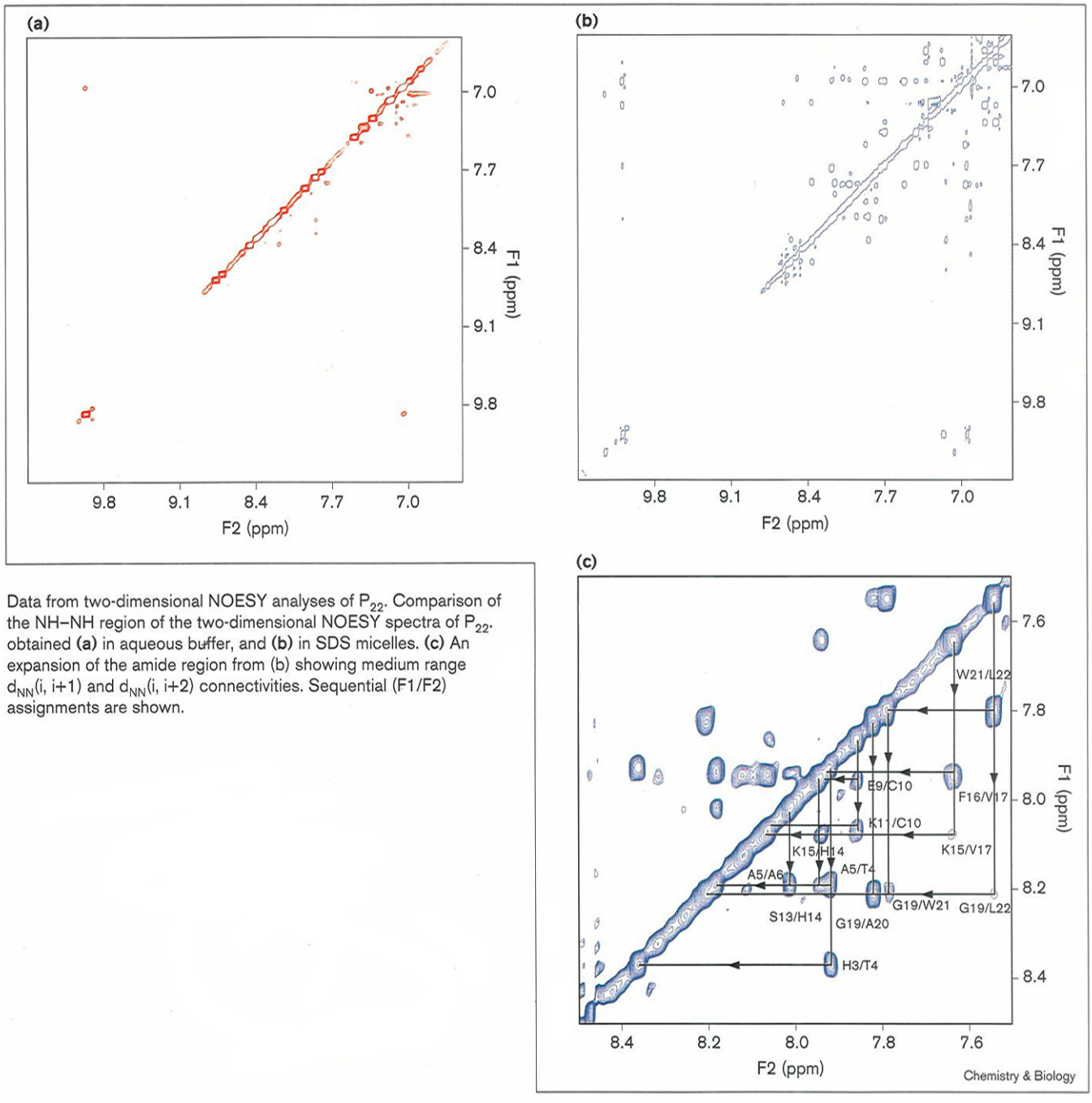

Data from two-dimensional NOESY analyses of P_{22}. Comparison of the NH–NH region of the two-dimensional NOESY spectra of P_{22} obtained **(a)** in aqueous buffer, and **(b)** in SDS micelles. **(c)** An expansion of the amide region from (b) showing medium range $d_{NN}(i, i+1)$ and $d_{NN}(i, i+2)$ connectivities. Sequential (F1/F2) assignments are shown.

better defined structure, although the increased line broadening introduced by the micellar environment makes extraction of accurate dihedral angles more difficult. The superposition of chemical shifts and line broadening in the presence of SDS therefore prevented the use of other parameters such as $^3J_{N\alpha}$ coupling constants, temperature coefficients for amide resonances, and $C_\alpha H$ chemical shift index [13] to derive additional information concerning the secondary structure. H/D exchange data were used either to identify slowly exchanging protons that result from hydrogen bonding in structured domains, or to determine if the peptide existed in an entirely random conformation.

Structures were analyzed for distance, angle and dihedral angle violations, and the NH–NH distances were computed for every residue (Figure 3). The observation of short NH–NH distances toward the carboxyl terminus provides support for a right-handed helical structure. Kabsch–Sander's method was used to classify the type of secondary structure observed [14]. Most structures (> 50%)

Figure 4

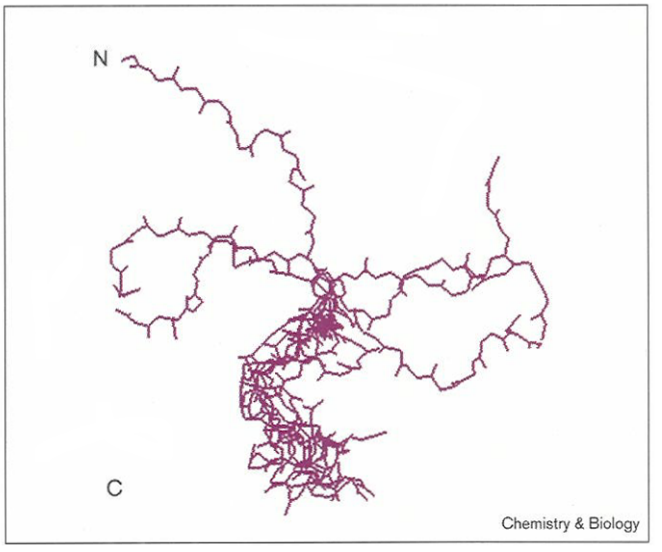

Structure of the free peptide. A family of seven structures aligned around the carboxyl terminus (from residues 10 to 22) is shown.

Figure 5

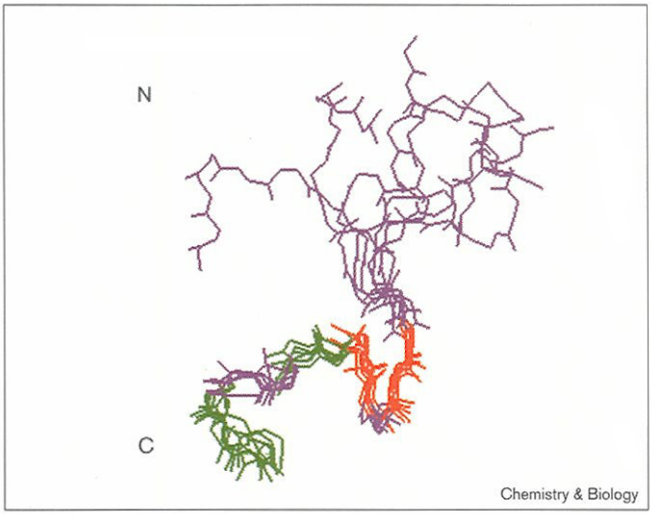

Structure of the SDS micelle bound peptide. A family of seven structures aligned at the structured carboxyl terminus (from residues 10 to 22) is shown, with positively charged residues in red, hydrophobic in green, and the neutral polar residues in mauve.

showed the presence of a Type-1-like turn near the carboxyl terminus. The absence of an overall tertiary fold in a peptide may contribute to the relatively high energy minima observed, due to the absence of additional interactions that stabilize such structures within a protein. In this regard, it is possible that the structure of the amino terminus of the perforin holoprotein may show some variations from the peptide described here, although we believe the model described herein to be valid for understanding the structural basis of perforin activity.

Structural features observed from NOE data and H/D exchange data

The structure of the peptide determined in the absence of SDS is flexible and exists mainly as a random coil (Figure 4). This is in contrast with the structure determined in the presence of SDS, which shows two distinct and well defined structurally ordered regions from residues 7 to 15 and at the carboxyl terminus (Figures 5 and 6). In SDS, the amino terminus of P_{22} is fairly disordered, whereas there is evidence for a Type-1-like turn in the carboxyl terminus of P_{22}. These structures have been generated from the experimental NOE constraints following a distance-geometry simulated-annealing protocol. One domain spans the middle of the peptide from residues 7 to 15, and contains a preponderance of positively charged residues, namely, Arg7, Lys11, Arg12, His14 and Lys15. Medium range $d_{\alpha N}$ (i, i+2) and $d_{\alpha N}$ (i, i+3) connectivities, and d_{NN}(i, i+1) cross-peaks, characteristic of a relatively ordered structure, are observed for the carboxy-terminal residues (Figure 7). In Figure 6, one hydrogen bond contact is seen between the carbonyl oxygen of Pro18 and the NH of Ala20. This supports the Type-1-like turn from residues 18 to 20.

The rationale for believing that the slower hydrogen exchange reflects hydrogen bonding stems from the fact that in water with no detergent hydrogen exchange is faster because the structure is less defined as a result of increased conformational flexibility in the absence of micelles (Figure 7). This residual structure is not observed in NOESY spectra (Figure 3a) because it is short-lived. For similar reasons, the better defined structure of the micelle-bound peptide gives rise to significant NOE patterns (Figure 3), whereas the absence of many hydrogen bond contacts in structures such as that shown in Figure 6 reflects minor structural fluctuations, with only one clear hydrogen bond contact as described immediately above. For this reason, the NH exchange data was not used to provide structural constraints during the distance-geometry calculation, to avoid the introduction of any structural bias. Based on these data, and the results of simulated-annealing calculations, the carboxyl terminus of P_{22} has an ordered structure that approximates a Type-1 turn.

The peptide exists in an overall random conformation in aqueous solution (Figure 4) as judged by the lack of NOE cross-peaks, in comparison to the experiments carried out in the presence of SDS (Figure 3a). Similar observations have been reported for structures of short membrane-spanning peptides in aqueous media [11]. It appears that a well defined structure is induced only in a membrane-like environment, consistent with previous observations of other membrane-spanning peptides (such as alamethicin and bacteriopsin) that have been studied in micellar solutions [15,16].

Figure 6

A stereo view of the domain described in Figure 5. Residues 18, 19 and 20, at the Type-1-like turn, are numbered.

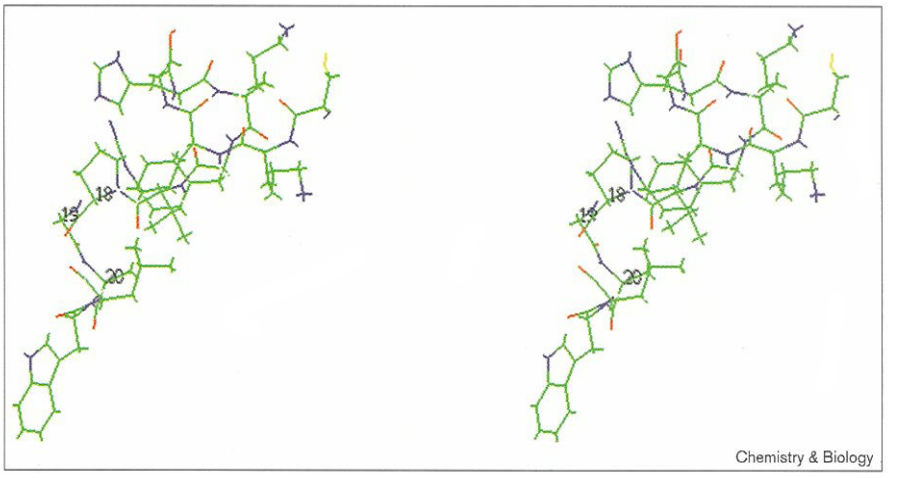

Structure–function relationships for peptide P_{22}

Many antimicrobial peptides are cationic [17] (for example, indolycidin [18], and magainin [19,20]), which suggests that a net positive charge is required for interaction with the negatively charged surface of a membrane bilayer (Figure 1). These positively charged peptides appear to possess membrane-perturbing ability, as previously observed for mellitin [21]. The central region of the peptide is positively charged, and perhaps forms a binding surface or groove for a negatively charged membrane. Although the backbone fold associated with the positively charged domain does not conform to any standard structure, it is observed that the positively charged residues lie in a turn and project outward towards a common face. Binding of several positively charged residues may weaken the membrane surface, enabling the insertion of the carboxyl terminus of the peptide into the membrane. Weakening of the membrane bilayer may also promote the uptake of other monomers, which would insert in a similar manner and lead to the formation of larger pores. A number of cationic peptides are capable of forming structures, based on either amphipathic helix or on β-sheet elements [22,23], that result in porin formation. Similarly, aggregation of monomeric perforin to form membrane-spanning pores has been observed at high concentrations using electron microscopy [6]. However, no evidence for aggregation of the P_{22} peptide has been observed under the experimental NMR conditions reported here, either in the presence or absence of SDS (at least 3 mM and 10 mM peptide concentrations, respectively), and no NOESY cross-peaks are observed from an aggregated species. Some linebroadening is introduced by binding to the SDS

Figure 7

Sequential NOEs and H/D exchange data for P_{22} in SDS micelles. The height of the bar indicates the relative strengths of NOEs, or rates of H/D exchange. The strengths of NOEs provide distance constraints that are used in modeling the structure.

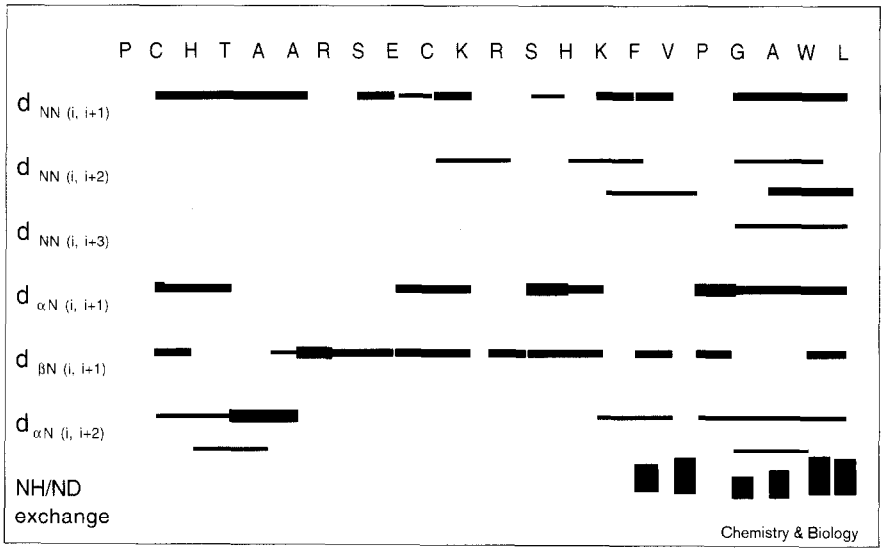

micelles, but not as a result of aggregation. The absence of significant aggregation under these experimental conditions is probably a reflection of several factors. Foremost among these, an SDS micelle is only an approximation of a phospholipid bilayer (albeit an approximation that is commonly made). As such, the micelle may not reflect the compositional or structural preference of the peptide. Because there is no available structure of the aggregate of either the peptide or full-length perforin bound in a phospholipid membrane, other than electron microscopy images of the perforin pore, only speculative suggestions can be made. For example, the pore may require a dimerization of peptides (as in the case of gramicidin [24]) to fully span the membrane. In the case of a micelle one does not have two solvent-exposed faces, and this may be one reason for the absence of aggregation. Also, the lack of aggregation is also promoted by the low peptide:micelle ratio of 1:1 (with ~80 SDS molecules per micelle). Overall, we believe the structure that we have determined may represent a snapshot of an isolated subunit of the perforin pore, which is inhibited from aggregating to form an active pore.

Complex formation with SDS micelles as a function of H/D exchange

Measurement of amide–proton exchange provides a method for evaluating the rates of complex formation between the peptide and SDS micelles. Following the procedure of Hammen *et al.* [25], the results of these experiments demonstrate that complex formation is rapid in comparison to the rate of proton exchange. Also, H/D exchange experiments indicate that several amide protons are more protected than others (Figure 7). In particular, the amide protons of Trp21, Val17, Leu22 and Phe16 are in slow exchange, Gly19 is in medium exchange, whereas the remaining amides were found to be in fast exchange with solvent protons. These results indicate that, although the peptide has a more rigid structure in the presence of SDS, the peptide is still generally exposed to solvent. The region of slow exchange lies toward the carboxyl terminus, which provides further support for the idea that this region is either shielded from the solvent, or that the amide protons may be involved in hydrogen bonding or formation of secondary structure. The same trend is observed in the absence of SDS micelles, although the peptide is seen to be more flexible based on the smaller number of NOE's observed in a NOESY experiment (Figure 3a), and the faster rate of NH/ND exchange. Although the overall structure remains fairly flexible, both the amide exchange data and the observed NOE's indicate that the carboxyl terminus is more structured than the amino terminus of the peptide in the presence of micelles.

Existence of alternative conformations for Trp21 in micelle-bound P_{22}

The one-dimensional ^1H spectrum of P_{22} shows two distinct chemical shifts for the imino proton of the indole ring in the presence of SDS micelles (Figure 2a), indicating that Trp21 can exist in two different conformational states (in a ratio of ~9:1 at 298K). Increasing the solution temperature facilitates rapid interconversion of the two conformers and the smaller signal is observed to coalesce into the more intense signal. The same phenomenon might be expected for other residues, but cannot be observed, presumably as a result of chemical shift overlap.

Significance

Secretion of perforin by killer lymphocytes is an initiating event in T-cell-mediated cell killing. Perforin monomers aggregate and form pores in target membranes, leading to a breakdown of the transmembrane osmotic gradient, and also allow other cytolytic mediators access to the target cell so that apoptosis can be initiated. The first 19 residues of perforin are sufficient for cytolytic activity, and the synthetic peptide P_{22} (residues 1–22) has been used as a 'model' for studying perforin structure and activity. Recent studies suggest that the gel state of the lipid chain rather than the head group is a determining factor for activity of holoperforin [26], while hydrogen bonding to cholesterol on membrane surfaces may also influence insertion and pore formation [27]. SDS micelles provide an interface between hydrocarbon and aqueous media, and have been used widely in NMR studies of membrane-binding peptides and other interfacial phenomena [15,16]. We have identified two structurally well defined regions of P_{22} in the presence of SDS micelles. One region forms a positively charged binding pocket for the negatively charged membrane. As a model for the lytic action of P_{22}, we propose that the strong electrostatic interaction weakens the membrane and facilitates insertion of the relatively neutral/hydrophobic stretch of P_{22}. Although other domains of perforin, distinct from the amino terminus, are known to contribute to its lytic function, this model provides insight into the initial steps of the lytic pathway. Finally, the structural model described here for perforin is likely to be relevant to understanding the mechanisms of other cationic antimicrobial peptides.

Materials and methods

Formation of the SDS–peptide complex

The 22-residue amino-terminal peptide of human perforin was synthesized as described by Rochel and Cowan [10]. SDS (37.3 mg) and P_{22} (4.3 mg) (80:1) were dissolved in deionized water. The high concentration of micelles ensures that there is at least one peptide per micelle [15,28]. Solutions of both SDS and the peptide were prepared separately in aqueous solution, and then mixed together. The resulting solution was initially observed to turn cloudy, but cleared within a few minutes, and was allowed to equilibrate overnight before spectral acquisition.

NMR experiments

NMR experiments were carried out on a Bruker Avance DMX spectrometer operating at 600.13 MHz. Data were collected at 25°C and processed using either Bruker's XWINNMR software, or Felix (Molecular Simulations, Inc.) operating on a silicon graphics station IRIX-4000.

For two-dimensional NMR measurements the sample contained 3 mM perforin P_{22} in either 90% H_2O/10% D_2O, or in 100% D_2O. The pH was adjusted to 5 for NOESY measurements, because low pH minimizes the rate of exchange among exchangeable protons. Two-dimensional NOESY and TOCSY experiments [29] were recorded using a sweep width of 8012.820 Hz in a phase sensitive mode. The NOESY spectra were recorded with mixing times of 100, 200, and 300 ms. A DQF–COSY spectrum was acquired with 768t1 increments and a sweep width of 6009.615 Hz. Presaturation was accomplished during the relaxation delay. Water presaturation for the NOESY and TOCSY experiments was achieved using a gradient pulse [30]. The number of complex points collected for TOCSY and NOESY spectra was 512 and 2048 in the t1 and t2 dimensions, respectively, and the spectra were apodized with a –3.00 Hz gaussian in t1, and a shifted sinebell in t2. Domain t1 was zero-filled to 1024 points.

For the H/D exchange experiments a TOCSY experiment with a short mixing time of 38 ms was run. To determine if the rate of complex formation was faster than the rate of NH exchange, the samples were prepared in two ways. First, the sample was taken up in the SDS solution, equilibrated overnight, and then lyophilized. Subsequently the sample was dissolved in D_2O before spectral acquisition. Alternatively, the sample was dissolved directly in an SDS solution made up in D_2O just prior to spectral acquisition. If complex formation was slower than the rate of exchange, then the two sets of data would yield different apparent exchange rates. This was not observed.

Resonance assignments were made based on the method described by Wuthrich [12]. The spin systems were first identified using DQF–COSY and TOCSY experiments, followed by sequential assignments of the residues using NH–NH connectivities.

Input restraints and starting structure of the complex

Input distance restraints were obtained from two-dimensional NOESY experiments recorded at 25°C for three different mixing times (100, 200 and 300 msec). The volume integrals of the NOESY peaks were converted to distance restraints using reference cross peaks calibrated to a known distance. The distance restraints were classified as strong, medium, or weak, and were assigned lower and upper bounds. Wherever a pseudo-atom was defined for a residue, a pseudo-atom correction was also included.

A set of chiral restraints were generated within the Insight II package. Because line-broadening in the presence of SDS micelles precluded the measurement of accurate coupling constants, and therefore accurate dihedral angles, the peptide structure was generated using 320 NOE distance constraints and the default dihedral angles associated with the force field. The DG/SA INSIGHT II package was also used to model the data.

The starting structure of the amino terminus of perforin was generated using the Insight II package (Molecular Simulations, Inc). The initial structure had a random conformation, this was further minimized using a CVFF force field until the energy was below 0.01 kcal/mole-Å. The minimized structure was then used in all distance geometry calculations.

Acknowledgements

This work was supported by the National Science Foundation (CHE-9706904). J.A.C. is a Camille Dreyfus Teacher–Scholar, and a National Science Foundation Young Investigator.

References

1. Lowin, B., Hahne, M., Mattmann, C. & Tschopp, J. (1994). Cytotoxic T-cell cytotoxicity is mediated through perforin and Fas lytic pathways. *Nature* **370**, 650-652.
2. Nicholson, D.W. & Thornberry, N.A. (1997). Caspases: killer proteases. *Trends Biochem. Sci.* **22**, 299-306.
3. Lichtenheld, M.G. & Podack, E.R. (1988). Structure and function of human perforin. *Nature* **355**, 448-451.
4. Lowin, B., Kraehenbuehl, O., Mueller, C., Dupuis, M. & Tschopp, J. (1992). Perforin and its role in T lymphocyte-mediated cytolysis. *Experientia* **48**, 911-920.
5. Lowin, B., Peitsch, M.C. & Tschopp, J. (1995). Perforin and granzymes: crucial effector molecules in cytolytic T lymphocyte and natural killer cell-mediated toxicity. *Curr. Top. Microbiol. Immunol.* **198**, 1-24.
6. Persechini, P.M., Ojicus, D.M., Adeodato, S.C., Notaroberto, P.C., Daniel, C.B. & Young, J.D.-E. (1992). Channel forming activity of perforin N terminus and a putative α-helical region homologous with complement C9. *Biochemistry* **31**, 5017-5021.
7. Ojicus, D.M., Persechini, P.M., Zheng, L.M., Notarobeto, P.C., Adeodato, S.C. & Young, J.D.-E. (1991). Cytolytic and ion channel-forming properties of the N terminus of lymphocyte perforin. *Proc. Natl Acad. Sci. USA* **88**, 4621-4625.
8. Liu, C.-C., Walsh, C.M. & Young, J.D.-E. (1995). Perforin: structure and function. *Immunol. Today* **16**, 194-201.
9. Liu, C.-C., Persechini, P.M. & Young, J.D.-E. (1994). Characterization of recombinant mouse perforin expressed in insect cells using the baculovirus system. *Biochem. Biophys. Res. Commun.* **201**, 318-325.
10. Rochel, N. & Cowan, J.A. (1996). Negative cooperativity exhibited by the lytic amino-terminal domain of human perforin: implications for perforin mediated cell lysis. *Chem. Biol.* **3**, 31-36.
11. Barnham, K.J., Monks, S.A., Hinds, M.G., Azad, A.A. & Norton, R.S. (1997). Solution structure of a polypeptide from the N terminus of the HIV protein Nef. *Biochemistry* **36**, 5970-5980.
12. Wuthrich, K. (1986). NMR of proteins and nucleic acids. Wiley-Interscience, New York.
13. Wishart, D.S., Sykes, B.D. & Richards, F.M. (1991). Relationship between nuclear magnetic resonance chemical shift and protein secondary structure. *J. Mol. Biol.* **222**, 311-333.
14. Kabsch, W. & Sander, C. (1983). Dictionary of protein secondary structure: pattern recognition of hydrogen-bonded and geometrical features. *Biopolymers* **22**, 2577-2637.
15. Pervushin, K.V., Arseniev, A.S., Kozhich, A.T. & Ivanov, V.T. (1991). 2D NMR study of the conformation of (34-65) bacteriopsin polypeptide in SDS micelles. *J. Biomol. NMR* **1**, 313-322.
16. Franklin, J.C., Ellena, J.F., Jayasinghe, S., Kelsh, L.P. & Cafiso, D.S. (1994). Structure of micelle-associated alamethicin from ^{1}H NMR. Evidence for conformational heterogeneity in a voltage-gated peptide. *Biochemistry* **33**, 4036-4045.
17. Gough, M., Hancock, R.E.W. & Kelly, N.M. (1996). Antiendotoxic potential of cationic peptide antimicrobials. *Infect. Immunol.* **64**, 4922-4927.
18. Falla, T.J., Karunaratne, D.N. & Hancock, R.E.W. (1996). Mode of action of the antimicrobial peptide Indolicidin. *J. Biol. Chem.* **271**, 19298-19303.
19. Matsuzaki, K., Sugishita, K.-I., and Fujii, N. (1995). Molecular basis for membrane selectivity of an antimicrobial peptide magainin 2. *Biochemistry* **34**, 3423-3429.
20. Blazyk, J., Hua, J., Hing, A. & Schaefer, J. (1994). How do magainins interact with neutral and acidic lipids. In *Peptides: Chemistry, Structure and Biology.* (Hodges, R.S. & Smith, J.A., eds), pp. 772-773, Escom, Leiden.
21. Yuan, P., Fisher, P.J., Prendergast, F.G. & Kemple, M.D. (1996). Structure and dynamics of mellitin in lysomyristol phosphatidylcholine micelles determined by nuclear magnetic resonance. *Biophys. J.* **70**, 2223-2238.
22. Gilbert, G.E. & Baleja, J.D. (1995). Membrane binding peptide from the C2 domain of Factor VIII formed an amphipathic structure as determined by NMR spectroscopy. *Biochemistry* **34**, 3022-3031.
23. Buchko, G.W., Rozek, A., Zhong, Q. & Cushley, R.J. (1995). Sequence-specific ^{1}H NMR assignments to secondary structure of a lipid-associating peptide from human apo C-I: an NMR study of an amphipathic helix motif. *Pept. Res.* **8**, 86-94.
24. Cowan, J.A. (1997). *Inorganic Biochemistry. An Introduction.* (2nd edn), pp. 143-146., Wiley-VCH, New York.
25. Hammen, P.K., Gorenstein, D.G. & Weiner, H. (1996). Amphiphilicity determines binding properties of three mitochondrial presequences to lipid surfaces. *Biochemistry* **35**, 3772-3781.
26. Rochel, N. & Cowan, J.A. (1997). Dependence of the lytic activity of the N-terminal domain of human perforin on membrane lipid composition. Implications for T-cell preservation. *Eur. J. Biochem.* **249**, 223-231.
27. Ojicus, D.M., Jiang, S., Persechini, P.M., Storch, J. & Young, J.D.E. (1990). Resistance to the pore-forming protein of cytotoxic T cells: comparison of target cell membrane rigidity. *Mol. Immunol.* **27**, 839-845.

28. Killian, J.A., Trouard, T.P., Greathouse, D.V., Chupin, V. & Lindblom, G. (1994). A general method for the preparation of mixed micelles of hydrophobic peptides and sodium dodecyl sulphate. *FEBS Lett.* **348**, 161-165.
29. Bax, A. & Davis, D.G. (1985). MLEV-17-based two-dimensional homonuclear magnetization transfer spectroscopy. *J. Magn. Reson.* **65**, 355-360.
30. Piotto, M., Saudek, V. & Sklenar, V. (1992). Gradient-tailored excitation for single-quantum NMR spectroscopy of aqueous solutions. *J. Biomol. NMR* **2**, 661-665.